Kinetic Analysis of Controlled/"Living" Radical Polymerizations by Simulations. 2. Apparent External Orders of Reactants in Atom Transfer Radical Polymerization

Devon A. Shipp[†] and Krzysztof Matyjaszewski*

Center for Macromolecular Engineering, Department of Chemistry, Carnegie Mellon University, 4400 Fifth Avenue, Pittsburgh, Pennsylvania 15213

Received September 28, 1999; Revised Manuscript Received December 30, 1999

ABSTRACT: Simulations of atom transfer radical polymerization (ATRP) have been used to examine the kinetics of these reactions. Because ATRP is subject to the persistent radical effect, the apparent external orders of various reactants are predicted to behave in a complex manner, generally not being simple first- or inverse-first orders. Addition of deactivating species at the beginning of the reaction results in the apparent external orders of the initiator and activator tending toward unity. Heterogeneity of the reaction system, where activator and/or deactivator may be only partially soluble, was also investigated. It was found that the ratio of soluble activator-to-soluble deactivator governed the rate of polymerization. The apparent external orders of the initiator and activator were found to be close to unity under the heterogeneous conditions simulated. Simulations of ATRP initiated with very efficient and fast initiators showed that these may lead to a substantial and irreversible buildup of deactivator species. This led to the conclusion that the rate of polymerization can be dependent upon the initiator used and, more generally, is dependent on the relative amount of deactivator available for reaction.

Introduction

Recent developments in controlling chain structure and functionality of polymers synthesized through free radical polymerization have exemplified the usefulness of controlled radical polymerizations (CRP).[1] A variety of materials, such as blocks copolymers, stars, telechelics, and (hyper)branched polymers, can be synthesized through such methods as atom transfer radical polymerization (ATRP),[2] nitroxide-mediated polymerization (NMP),[3] and degenerative transfer techniques (iodide-mediated[4] and reversible addition−fragmentation chain transfer (RAFT) polymerization[5]). These techniques can also synthesize linear polymer chains that have predictable molecular weights ($M_n = M_0 \times DP_n = M_0 \times$ conversion $\times [M]_0/[In]_0$, where M_0 is the molecular weight of the monomer repeat unit and $[M]_0$ and $[In]_0$ are the initial concentrations of the monomer and initiator (or in the case of RAFT, the transfer agent), respectively) and relatively narrow polydispersities ($M_w/M_n < 1.5$) under appropriate conditions.

The basic premise of ATRP and other CRPs is that all chains, of concentration $\sim 10^{-1}-10^{-3}$ M, are initiated at low monomer conversions. However, the actual concentration of active species (free radicals) is kept much lower than the total concentration of chains (approximately $10^{-7}-10^{-8}$ M) by the dynamic equilibrium that is established between dormant (P_nX) and active chains ($P_n^\bullet$), as shown in Scheme 1 for ATRP.[2] This transfer of the halogen atom (X) within the equilibrium is catalyzed by a transition metal/ligand complex (Mt^nY/L). This results in only a small percentage of chains undergoing irreversible radical−radical termination that removes the functionality from the chain ends. However, this small amount of termination leads to a buildup of excess deactivator ($XMt^{n+1}Y/L$), thus favoring deactivation further over radical−radical termination and thereby enhancing control. This scenario is termed the persistent radical effect and has been shown by Fischer,[6,7] and ourselves,[8] to be operating in both ATRP and NMP.

Scheme 1

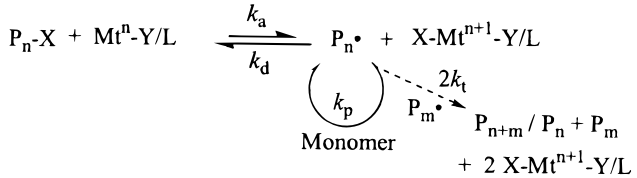

The kinetics of the reactions, and also the concentrations of the species involved, obviously play an important role in the extent of control exhibited in controlled/"living" polymerizations, and there have been several reports of the experimental determination of the apparent external orders of the reactants in ATRP.[9−12] For various monomers and reaction conditions, the apparent external orders of the reactants were often found to be fractional. In the Cu^IBr (or Cu^ICl)/dNbpy-mediated ATRP of styrene, it was found that the polymerization was first-order with respect to initiator and activator, while a nonlinear dependence was found for the deactivator.[9] For Cu^IBr/dNbpy-mediated ATRP of methyl methacrylate (MMA) (dNbpy = 4,4′-di(5-nonyl)-2,2′-bipyridine), similar results were obtained.[10] In contrast, methyl acrylate (MA) polymerization under similar conditions showed noninteger orders (0.8 in initiator, −1 in deactivator, and nonlinear in activator).[11] Percec et al.[12] found that in the ATRP of styrene and MMA the polymerizations were 0.8-order in Cu^ICl and for MMA 0.37-order in initiator. Pascual et al.[13] observed the apparent zero external order for initiator in styrene ATRP mediated by Cu^ICl/bpy in 10% dimethylformamide.

It is clear from these experimental data that the apparent external orders of the reactants are complicated. The goal of this paper is to examine the apparent

* To whom correspondence should be addressed.
[†] Current address: Department of Chemistry, Clarkson University, Potsdam, NY 13699-5810.

10.1021/ma991651m CCC: $19.00
Published on Web 02/08/2000

Scheme 2

Initiation

$$R\text{-}X + Cu^{I}X/L \underset{k_{d0}}{\overset{k_{a0}}{\rightleftharpoons}} R\bullet + Cu^{II}X_2/L$$

$$R\bullet + M \xrightarrow{k_i} P_1\bullet$$

$$3\,M \xrightarrow{k_{therm}} 2\,R\bullet$$

Propagation

$$P_n\text{-}X + Cu^{I}X/L \underset{k_d}{\overset{k_a}{\rightleftharpoons}} P_n\bullet + Cu^{II}X_2/L$$

$$P_n\bullet + M \xrightarrow{k_p} P_{n+1}\bullet$$

Termination

$$2\,R\bullet \xrightarrow{k_{t0}} D_2$$

$$P_n\bullet + P_m\bullet \xrightarrow{k_{tc}} D_{n+m}$$

$$P_n\bullet + P_m\bullet \xrightarrow{k_{td}} D_n + D_m$$

$$P_n\bullet + R\bullet \xrightarrow{k_{tP}} D_n$$

Chain Transfer

$$P_n\bullet + M \xrightarrow{k_{tr,M}} D_n + R\bullet$$

external orders of the reactants through simulations of ATRP and to observe what effect altering key rate parameters has on the polymerization kinetics and amount of control observed. Our previous publication examined the effect that the diffusion dependence of radical−radical termination has on the kinetics of ATRP.[8]

Simulation Technique

The Predici program[14] was used for the simulations. Several previous studies have shown that the package is versatile enough to allow the incorporation of many reactions.[14−18] Predici uses a discrete h−p method to represent chain length distributions and an adaptive Rothe method as a numerical strategy for time discretization. Predici is especially convenient for simulations of "stiff" systems in which concentrations of reagents and rate constants of the involved reactions differ by several orders of magnitude. Concentrations of all species, as well as the distributions of all polymeric species, can be followed. The model used is for $Cu^{I}X$/$Cu^{II}X_2$-mediated ATRP, as given in Scheme 2,[8] but is general for other metal catalysts. Values for each rate constant (or coefficient) are given in Table 1 and were taken from the literature.[19−25] For the simulations that included precipitation reactions the model outlined in

Table 1. Parameters Used in ATRP Simulations[a]

parameter	value	ref
k_i (L mol^{-1} s^{-1})	16000	19, 20
k_p (L mol^{-1} s^{-1})	1600	21
$2k_{tc}(0)$ (L mol^{-1} s^{-1})	1×10^9	19
$2k_{td}(0)$ (L mol^{-1} s^{-1})	1×10^8	19
$2k_{t0}$ (L mol^{-1} s^{-1})	5×10^9	19
$k_{tr,M}$ (L mol^{-1} s^{-1})	0.22	22
k_d (k_{d0}) (L mol^{-1} s^{-1})	1.1×10^7	23
k_a (k_{a0}) (L mol^{-1} s^{-1})	0.45	23
k_{tP} (L mol^{-1} s^{-1})	1×10^9	19, 24
k_{therm} (L^2 mol^{-2} s^{-1})[b]	0 or 4.8×10^{-11}	25
$[M]_0$ (M)	4.3	
$[RX]_0$ (M)	0.045	
$[Cu^{I}X]_0$ (M)	0.045	
$[Cu^{II}X_2]_0$ (M)	0	
temperature (°C)	110	

[a] Some parameters varied in some simulations. See text and figure captions. [b] $k_{therm} = 0$ for simulations presented in Figures 1−6 and 8−12, while $k_{therm} = 4.8 \times 10^{-11}$ L^2 mol^{-2} s^{-1} for simulations presented in Figure 7.

Scheme 3

$$(Cu^{I}\text{-}X/L)_{sol} \underset{k_{sol}}{\overset{k_{insol}}{\rightleftharpoons}} (Cu^{I}\text{-}X/L)_{insol}$$

$$(Cu^{II}\text{-}X_2/L)_{sol} \underset{k_{sol}}{\overset{k_{insol}}{\rightleftharpoons}} (Cu^{II}\text{-}X_2/L)_{insol}$$

Scheme 3 was adopted. The conversion and chain length dependence of $k_t(DP,C)$ was calculated using the interpreter function of Predici. For each time step, the degree of polymerization was calculated using $DP = C([M]_0/[RX]_0)$, where C is the fractional conversion of monomer to polymer. Note that DP is dependent upon $[RX]_0$ at a given conversion; this means that $k_t(DP,C)$ will behave differently in simulations where $[RX]_0$ is altered. Using this DP, $k_t(DP,C)$ was then calculated using eq 1,

$$k_t(DP) = k_t(0)(DP)^{-(0.65+C)} \quad (1)$$

which is based on work of Griffith et al.,[26] with the $k_t(0)$ value given in Table 1. For simulations of 50% solution ATRP experiments, the exponent in eq 1 was $-(0.65 + C)$. Calculations were performed on a personal computer (two 300 MHz processors) running Windows NT and took approximately 2−10 min to complete.

Results and Discussion

Model Development. We have used computer simulations to investigate in a systematic manner the apparent external orders of the main reactants. This allows each reactant or rate constant to be altered simply and the effect on the polymerization to be ascertained. However, simulations are reliant on the development of an accurate model and the availability of rate data. The major reactions in ATRP have been identified, particularly for styrene polymerization at 110 °C with $Cu^{I}Br$/dNbpy catalyst.[9] In this case, the activation and deactivation rates have been determined,[9,23] as well as propagation rate constants,[21] and side reactions observed.[9,27] Previously we used the model given in Scheme 2 to simulate ATRP when investigating the effect that a chain length and viscosity-dependent termination rate coefficient ($k_t(DP,C)$) has on the polymerization.[8] Simulations using this model were reason-

ably successful in reproducing polymerization rates, species concentrations, and polymer properties (number-average molecular weight, M_n, and polydispersity, M_w/M_n). We again use this same model, including the chain length and viscosity dependent $k_t(DP,C)$ with the appropriate rate constants/coefficients and concentrations given in Table 1.

Equation 2 describes the rate of polymerization in

$$\ln\left(\frac{[M]_0}{[M]}\right) = k_p \frac{k_a}{k_d} \frac{[RX][Mt^n]}{[XMt^{n+1}]} t \qquad (2)$$

ATRP.[9] It predicts that the rate of polymerization is first-order in both initiator and activator and inverse first-order for the deactivator. If initiation is quantitative, a fast preequilibrium exists, and radical−radical termination is negligible; the [RX], [Cu^IX], and [$Cu^{II}X_2$] terms do not change and therefore can be replaced with $[RX]_0$, $[Cu^IX]_0$, and $[Cu^{II}X_2]_0$ (i.e., initial concentrations). If the apparent external orders are found by altering $[RX]_0$, $[Cu^IX]_0$, or $[Cu^{II}X_2]_0$, then any changes in the concentrations of these species (especially $[Cu^{II}X_2]$ because it often starts at zero) during the reaction will lead to a situation where the apparent external orders may not behave according to eq 2. For both styrene and MMA,[9,10] our experimental results were in agreement with eq 2 with respect to $[RX]_0$ and $[Cu^IX]_0$; however, the inverse first-order in $[Cu^{II}X_2]_0$ was not found. Other data for MA, MMA, and styrene did not agree with the predicted orders from eq 2.[11−13]

The complicated kinetics that have been observed in ATRP potentially stem from a variety of factors. One principal reason is that ATRP is subject to the persistent radical effect, which Fischer has shown predicts that the evolution of deactivator occurs throughout the polymerization, if a constant termination rate coefficient is assumed, and therefore the first-order kinetic plot of monomer consumption is curved.[6,7] However, we have shown that inclusion of diffusion-controlled termination results in a nearly linear $\ln([M]_0/[M])$ vs time plots, which are normally observed experimentally.[8] Fischer's kinetic analysis of the persistent radical effect resulted in eqs 3−5

$$\ln\left(\frac{[M]_0}{[M]}\right) = \frac{3}{2}k_p([RX]_0[Mt^n]_0)^{1/3}\left(\frac{k_a}{3k_d 2k_t}\right)^{1/3} t^{2/3} \qquad (3)$$

$$[P^\bullet] = ([RX]_0[Mt^n]_0)^{1/3}\left(\frac{k_a}{3k_d 2k_t}\right)^{1/3} t^{-1/3} \qquad (4)$$

$$[XMt^{n+1}] = ([RX]_0[Mt^n]_0)^{2/3}\left(\frac{3k_a{}^2 2k_t}{k_d{}^2}\right)^{1/3} t^{1/3} \qquad (5)$$

which describe the monomer, radical, and deactivator concentrations for ATRP.[7] From eq 3 it is clear that the rate of polymerization depends on the concentrations of initiator and activator in a complex manner. Furthermore, the deactivator does not even appear in eq 3 although it can be and has been directly measured.[28] In fact, eqs 2 and 3 are quite compatible if one takes into account the formation of deactivating species (XMt^{n+1}) during ATRP. Other possible reasons why the kinetics are complex include reaction mixture heterogeneity or variations in initiator efficiency. These are discussed in further detail below.

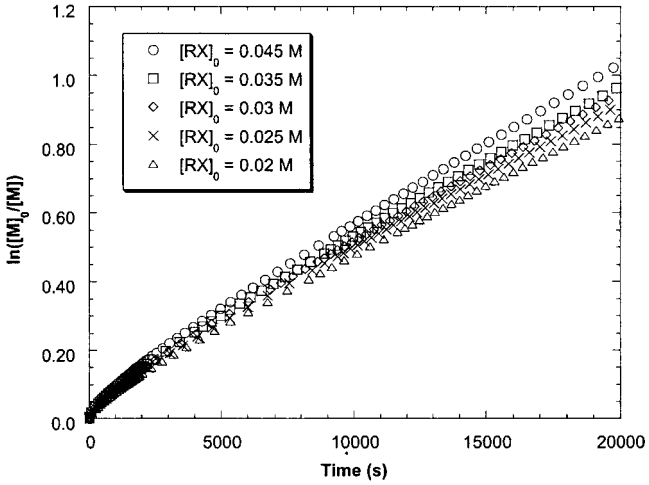

Figure 1. First-order kinetic plots of monomer consumption for ATRP of styrene with various $[RX]_0$. Other parameters as given in Table 1 except $k_{therm} = 0$.

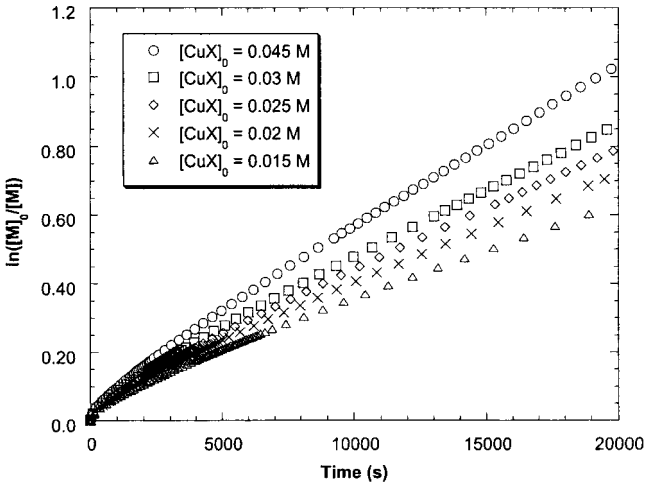

Figure 2. First-order kinetic plots of monomer consumption for ATRP of styrene with various $[Cu^IX]_0$. Other parameters as given in Table 1 except $k_{therm} = 0$.

Order of Initiator, Activator, and Deactivator. Figure 1 shows the first-order kinetic plot for styrene ATRP simulations as initiator concentration, $[RX]_0$, is altered and with the other parameters as given in Table 1. $[RX]_0$ is the only parameter that is changed in each simulation. As $[RX]_0$ is increased, the rate of polymerization also increases. Also, the shape of each plot is not strictly linear. This stems from the finite amount of termination occurring at early stages of the polymerization, but as molecular weight and conversion increase, the amount of termination, and hence curvature, tends to decrease.

The first-order kinetic plot for styrene ATRP simulations as $[Cu^IX]_0$ is altered is shown in Figure 2. Again, all parameters are as given in Table 1, with only $[Cu^IX]_0$ changing this time. As $[Cu^IX]_0$ is decreased, so is the rate of polymerization. As observed above, the first-order kinetic plots appear to have some curvature as a result of the increase in concentration of the deactivator by irreversible radical−radical termination. They are, however, reasonably linear after approximately 2500 s. Although the range of $[Cu^IX]_0$ used in the simulations shown in Figure 2 is similar to the range of $[RX]_0$ in Figure 1, it is clear that altering the catalyst concentration apparently has a more marked effect on the rate

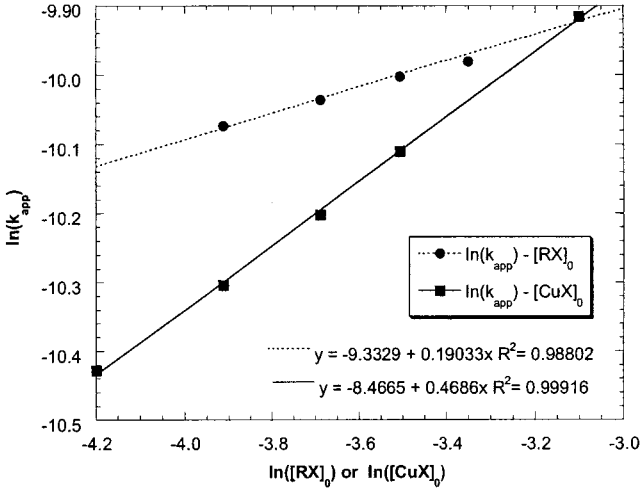

Figure 3. Plots of $\ln(k_{app})$ as a function of $\ln([RX]_0)$ or $\ln([Cu^IX]_0)$ obtained from fitting data in Figures 1 and 2.

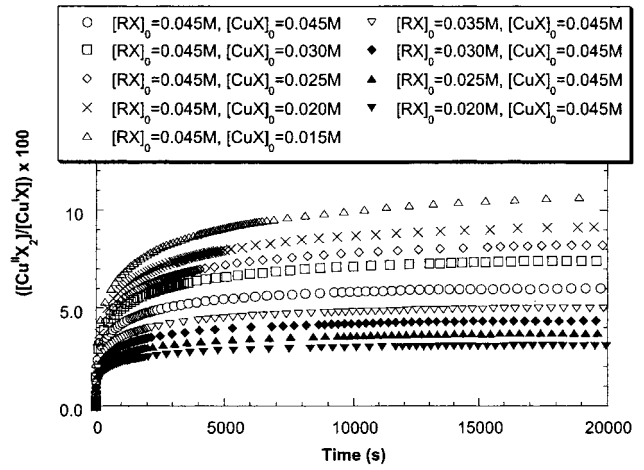

Figure 4. Percentage of $Cu^{II}X_2$ generated relative to Cu^IX with various $[RX]_0$ and $[Cu^IX]_0$ values (from the same simulation used to generate Figures 1 and 2).

of polymerization (i.e., the apparent external reaction order is larger).

Each of the plots in Figures 1 and 2 was fitted with a linear curve, the slope of which is equal to an apparent rate constant of polymerization ($k_{app} = d\ln([M])/dt$). From these data, Figure 3, being a plot of $\ln(k_{app})$ as a function of both $\ln([RX]_0)$ and $\ln([Cu^IX]_0)$, was constructed. Both data sets ($\ln([RX]_0)$ and $\ln([Cu^IX]_0)$) show linear behavior over the range of concentrations used in the simulations. (These concentrations are also typical of what are used experimentally.) However, the slopes of the linear fits, which are a measure of the external order of the particular reactant, are fractional and, as alluded to above, quite different from each other.

This difference is due to the varying amounts of termination that may occur at the very early stage of the reaction. That is, when $[RX]_0$ is altered, the ratio of $[Cu^{II}X_2]/[Cu^IX]$ changes in the opposite sense when compared with a variation in $[Cu^IX]_0$, as seen in Figure 4. These trends have their origin in several factors such as the concentration of primary radicals generated and the conversion and chain length dependent k_t (since this depends, in part, on $[RX]_0$). Such factors influence the ratio of $[Cu^{II}X_2]/[Cu^IX]$, which in turn alters k_{app}. The end result is that when $[RX]_0$ is changed, the effect on k_{app} is not as great as when $[Cu^IX]_0$ is altered.

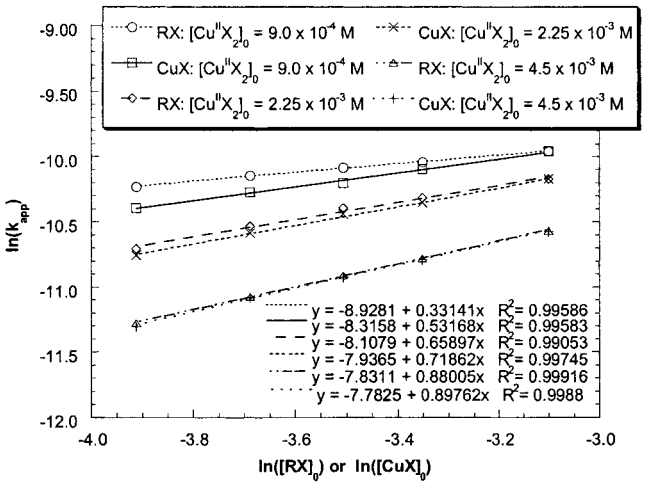

Figure 5. Plots of $\ln(k_{app})$ as a function of $\ln([RX]_0)$ or $\ln([Cu^IX]_0)$ with $[Cu^{II}X_2]_0$ as given on the plot ($k_{therm} = 0$).

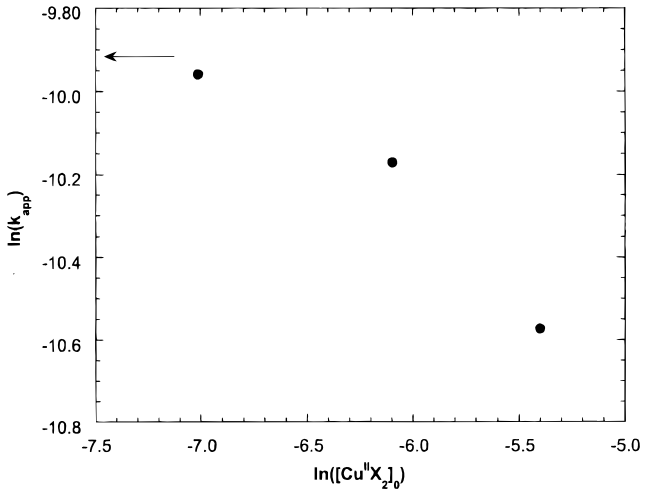

Figure 6. Plots of $\ln(k_{app})$ as a function of $\ln([Cu^{II}X_2]_0)$. Data are taken from the same simulations as presented in Figure 5. The arrow indicates the value of $\ln(k_{app})$ for $[Cu^{II}X_2]_0 = 0$ M.

Another series of simulations were performed, this time with finite concentrations of the deactivating $Cu^{II}X_2$ species present at the beginning (9×10^{-4}, 2.25×10^{-3}, and 4.5×10^{-3} M), and then $[RX]_0$ and $[Cu^IX]_0$ were varied in the same manner as above. This was done because in the laboratory it is difficult to completely avoid even small amounts (a couple of percent) of oxidized catalyst being present in the starting materials. The plots of $\ln(k_{app})$ as a function of both $\ln([RX]_0)$ and $\ln([Cu^IX]_0)$, with various initial concentrations of $Cu^{II}X_2$, are shown in Figure 5. For both $[RX]_0$ and $[Cu^IX]_0$ sets of conditions, increasing $[Cu^{II}X_2]_0$ leads to increasing apparent external orders, which appear to converge toward unity. Furthermore, plotting $\ln(k_{app})$ vs $\ln([Cu^{II}X_2])$, as shown in Figure 6, gives a nonlinear plot. This is because $Cu^{II}X_2$ is irreversibly produced during the polymerizations to an extent that varies between each reaction condition.

These data indicate that the rate of polymerization may not be externally first-order with respect to RX, Cu^IX, or $Cu^{II}X_2$. The apparent external orders of these reactants are far more complicated, even in apparently homogeneous systems, depending upon a priori initial concentrations, rates of activation, deactivation, initiation, and termination. It is therefore no surprise that

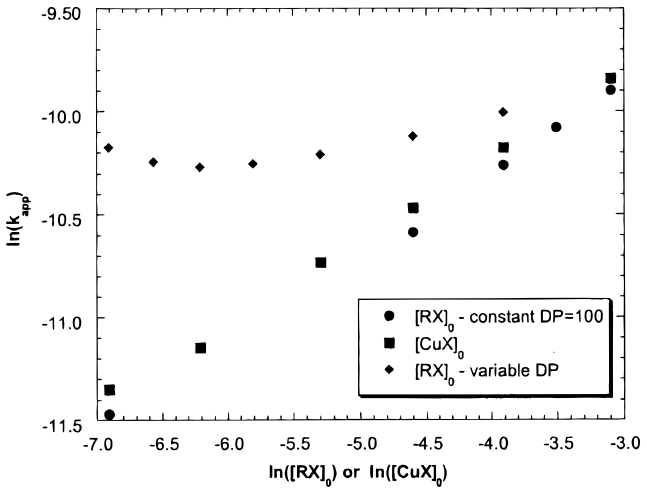

Figure 7. Plots of $\ln(k_{app})$ as a function of $\ln([RX]_0)$ or $\ln([Cu^IX]_0)$ obtained from fitting first-order kinetic plots of monomer consumption when thermal self-initiation is included in the simulation: (◆, ■) eq 1 used to calculate $k_t(DP,C)$; (●) eq 1 used to calculate $k_t(DP,C)$ but with DP = 100 in each simulation.

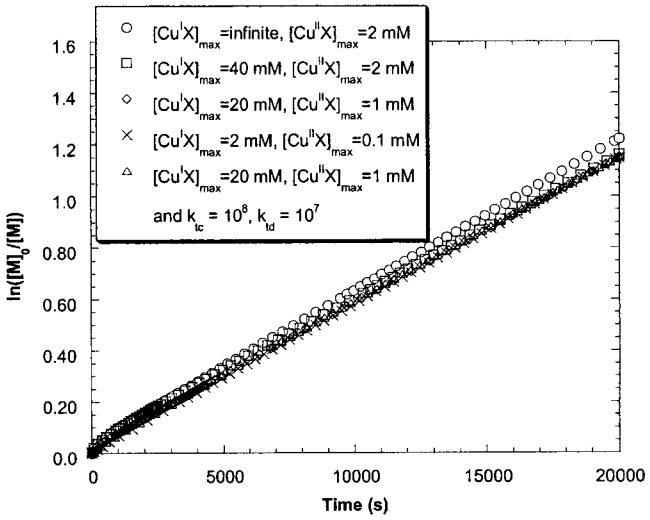

Figure 8. First-order kinetic plots of monomer consumption for ATRP of styrene for various limits of Cu^IX and $Cu^{II}X_2$ solubilities. Other parameters as given in Table 1 except $k_{therm} = 0$.

experimentally determined apparent external orders found in the literature thus far vary greatly. However, eq 2 does fully describe the rate of polymerization given that none of the reactant concentrations change (i.e., at any given short time slice). Equation 3, on the other hand, describes the rate of polymerization in terms of starting concentrations but assumes a constant termination rate.

It is worth noting that the rate of polymerization is very dependent upon $[Cu^{II}X_2]_0$ and the rate/extent at which the $Cu^{II}X_2$ evolves. Only a few percent of $Cu^{II}X_2$ in the Cu^IX sample, or produced through insufficient deoxygenation, is enough to alter the kinetics of the reaction and therefore also the observed external orders of the reactants. Also, the amount of $Cu^{II}X_2$ formed in the initial stages of the polymerization depends on the order of addition of reagents, mixing, etc., as already observed experimentally.[9]

Another phenomenon that occurs during polymerizations of styrene is self-initiation. This has been neglected in the above analysis so as to make the conclusions more general. However, it is instructive to include thermal self-initiation of styrene in the model and examine what effect it has on the kinetics of ATRP since it is known that this reaction is the driving force behind the kinetics of TEMPO-mediated controlled/"living" radical polymerization of styrene.[15] We have used data taken from Hui and Hamielec,[25] but as we pointed out earlier,[8] the rate constants obtained in their work are dependent on their model (which included a conversion-dependent termination rate coefficient). Therefore, using a rate constant for the thermal initiation of styrene from their work in the context of our model is not entirely satisfactory. However, due to the lack of alternatives we use the value obtained from Hui and Hamielec.

Figure 7 shows the plots of $\ln(k_{app})$ vs both $\ln([RX]_0)$ and $\ln([Cu^IX]_0)$ (diamonds, squares). The most obvious trend is that the apparent order for $[RX]_0$ is nonlinear, and $\ln(k_{app})$ increased when $\ln([RX]_0) < -6.2$ (i.e., $[RX]_0 < 0.002$ M). Contrary to this behavior, $\ln(k_{app})$ decreases in a linear fashion as $\ln([Cu^IX]_0)$ decreases. Similar trends have been observed experimentally by Pascual et al.[13] during homogeneous ATRP with Cu^ICl/bpy and 10% (v/v) dimethylformamide. These observations, while qualitatively agreeing with some experimental data, seem strange. Further simulations (circle symbols in Figure 7) with $[RX]_0$ being altered but the DP calculated using $[M]_0/[RX]_0 = 100$ (i.e., constant) showed a linear relationship very similar to that obtained for when $[CuX]_0$ was altered. It therefore appears (not surprisingly) that the extent to which termination rate coefficient is conversion dependent greatly affects the apparent rate of polymerization. (Note that when the apparent orders of $[CuX]_0$ are investigated, DP remains constant at 100; therefore, such behavior is not observed in this case.)

Inhomogeneity. As mentioned above, it is quite possible that not all the activator and/or deactivator are present in solution at the concentrations expected on the basis of the amount of Cu^IX added. In other words, it is possible that the reactions are heterogeneous, even though they may appear homogeneous to the eye. An example might be hypothetical dimeric copper species in the ATRP of MMA catalyzed by Cu^IBr/2dNbpy.[10] Furthermore, with the progress of the reaction and monomer consumption, the medium changes and consequently the solubility of reagents may change as well. To examine the effect a heterogeneous system would have on the kinetics of ATRP, we have included a precipitation reaction into the model. This has been done for both Cu^IX and $Cu^{II}X_2$ species, where an equilibrium between soluble and insoluble species (Scheme 3; $k_{sol} = k_{insol} = 10^3\ s^{-1}$) is established once the total concentration of the species reaches a limiting solubility concentration ($[Cu^IX]_{max}$ or $[Cu^{II}X_2]_{max}$). The insoluble species do not take part in any other reactions. However, the extent of heterogeneity is not known experimentally, so the simulations presented here have various solubility limits for both Cu^IX and $Cu^{II}X_2$ (although it is expected that Cu^IX will be more soluble in the organic media than $Cu^{II}X_2$, and so the limits reflect this difference). The choice of k_{sol} and k_{insol} was made such that the dynamics were fast, thereby not affecting the concentrations of the soluble/insoluble activator/deactivator species. Variations in these rate constants showed no change in the other data as long as $k_{sol} = k_{insol} > 10^3\ s^{-1}$.

Presented in Figure 8 are the first-order kinetic plots

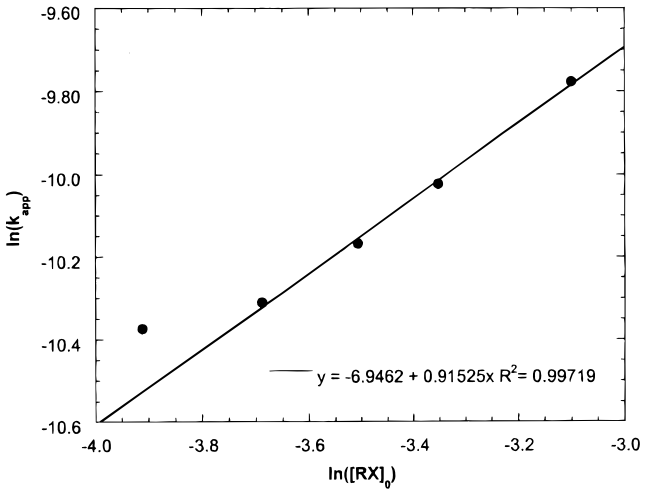

Figure 9. Plots of $\ln(k_{app})$ as a function of $\ln([RX]_0)$ for simulations of styrene ATRP for limited Cu^IX and $Cu^{II}X_2$ solubilities ($[Cu^IX]_{max} = 20$ mM, $[Cu^{II}X_2]_{max} = 1.0$ mM; $k_{therm} = 0$). Curve fit through data points for the four highest $[RX]_0$ used only.

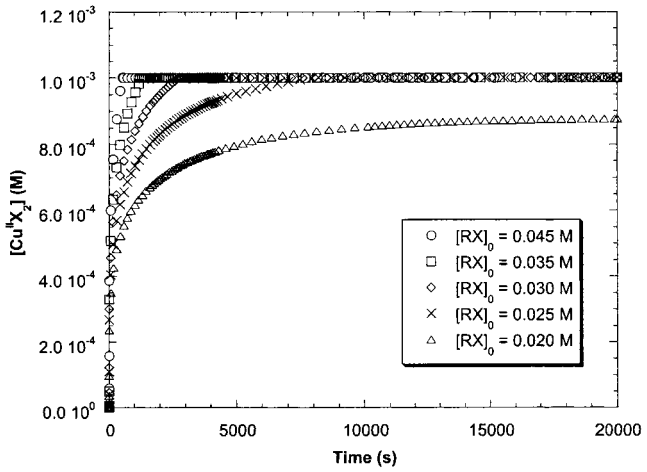

Figure 10. $[Cu^{II}X_2]$ as a function of time in simulations of styrene ATRP for various $[RX]_0$ and limited Cu^IX and $Cu^{II}X_2$ solubilities ($[Cu^IX]_{max} = 20$ mM, $[Cu^{II}X_2]_{max} = 1.0$ mM; $k_{therm} = 0$).

obtained from the simulations of styrene ATRP (50% solution) using the parameters given in Table 1 along with limited solubilities of Cu^IX and $Cu^{II}X_2$ as given in the figure. The simulation that had termination rate constants ($k_{tc} = 10^8$ M^{-1} s^{-1}, $k_{td} = 10^7$ M^{-1} s^{-1}) gave a linear first-order kinetic plot. (Rate constants were examined because inhomogeneity would result in linear first-order kinetics.) This is because the amount of deactivator available to react with the radicals, and thus form a dormant chain, is constant even though there is continual irreversible radical−radical termination. Further simulations were performed using a constant solubility limit for both Cu^IX and $Cu^{II}X_2$ ($[Cu^IX]_{max} =$ 20 mM and $[Cu^{II}X_2]_{max} = 2$ mM), $k_t(DP,C)$ described by eq 1 and only varying the initiator concentration (as was done above to determine the apparent external order for RX). Figure 9 shows the plot of $\ln(k_{app})$ vs $\ln([RX]_0)$ from the data obtained. Interestingly, all but the data point for the lowest $[RX]_0$ lie on a straight line, giving an apparent external order of close to 1. The reason for this behavior can be seen in Figure 10. This figure shows the deactivator concentration for these simulated experiments. For the highest $[RX]_0$, there is more deactivator generated because of the higher radical concentration which leads to more irreversible termination. Once $[Cu^{II}X_2]$ reaches the solubility limit, the concentration of deactivator available for reaction with the radical species remains constant, therefore effectively removing the influence of the persistent radical effect. For the lower $[RX]_0$, the amount of deactivator produced is actually lower than the solubility limit, resulting in the rate being more controlled by the persistent radical effect (i.e., less dependent on $[RX]_0$). It has to be stressed that eq 2 is obeyed from very early stages of the polymerization and continues to do so until the very end if *actual* but not *initial* concentrations of all reagents are used (RX corresponds to the dormant chain ends).

This section of work highlights the sensitivity of kinetic parameters on the activity of the catalyst and deactivator. The activity may be reduced by either insolubility or dimer (or higher aggregates) formation. While some ATRP systems clearly give heterogeneous systems (e.g., unsubstituted bpy, linear amines),[29,30] other ligands provide an apparently homogeneous reaction mixtures.[9,31] However, exactly how homogeneous these systems are and the exact nature of the activator and deactivator are still being sought.

Effect of Initiation Efficiency. The initiator has been shown to have a marked effect on the rate of ATRP, especially for MMA. It has been found for the ATRP of MMA that, of alkyl halide initiators, tertiary structures provide faster initiators than secondary, which in turn are faster than primary alkyl halides.[32] One group of very efficient initiators are sulfonyl halides, which have been proposed to be a "universal class of functional initiator" for ATRP.[12] This stems from the relatively fast initiation of these initiators for acrylate, methacrylate, and styrene polymerizations and the lack of substituent effects on the reactivity of the sulfonyl radical.

However, it has been noted that there is some variability in the rates of ATRP when very reactive initiators are used. In particular, variations in rate and apparent $Cu^{II}X_2$ formation are observed depending on the mode and rate of initiator addition. For example, if benzhydryl chloride is added quickly to a reaction mixture, then the color will change quickly from deep red/brown (typical of Cu^IX/2dNbpy species) to green (typical of $Cu^{II}X_2$/dNbpy), and the polymerization does not proceed or does so at an extremely slow rate.[32] On the other hand, if the initiator is diluted and added relatively slowly to the reaction vessel, then the polymerization occurs with a reasonable rate and in a controlled manner. Similar observations have been noticed for malonate initiators.[32]

We have investigated this phenomenon through a series of ATRP simulations. This was simply done by varying the activation rate of the initiator to the initiating radical. Figure 11 shows the first-order kinetic plot for monomer consumption from simulations of ATRP with various k_{a0} values. Clearly, the rate of polymerization is dramatically affected by the variations in k_{a0}. From Figure 12, which is a plot of the deactivator $Cu^{II}X_2$ concentration with time, it is apparent that increases in k_{a0} lead to more $Cu^{II}X_2$ being generated very early in the reaction and thus lead to a lower rate of polymerization. In fact, at the highest k_{a0} used, so much deactivator is produced that the radical concentration is lowered to a point where termination events are negligible, as indicated by the virtually constant $Cu^{II}X_2$ concentration throughout the remainder of the simulated reaction.

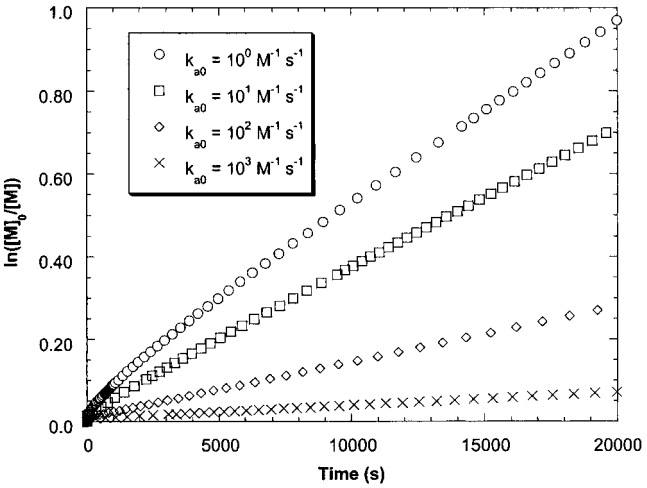

Figure 11. First-order kinetic plots for monomer consumption when k_{a0} is varied. Other parameters as given in Table 1 except $k_{therm} = 0$.

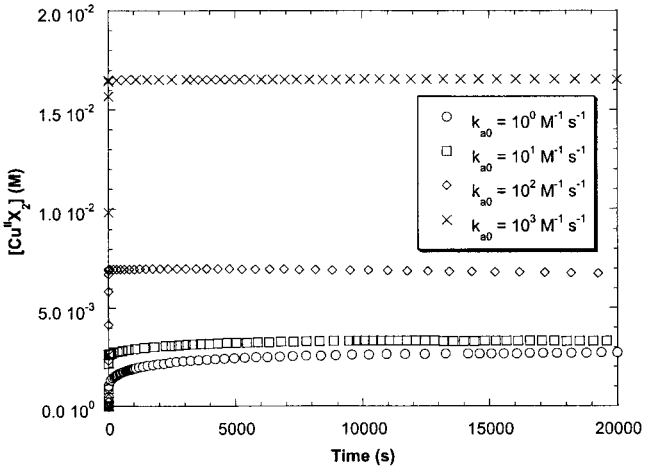

Figure 12. [$Cu^{II}X_2$] development during ATRP of styrene when k_{a0} is varied. Other parameters as given in Table 1 except $k_{therm} = 0$.

The extent of termination can be reduced by slow addition of the initiator so that there is a lower concentration of initiating radicals formed at any one time. This method has been used effectively for other very active initiators, such as benzhydryl chloride.[32] A corollary of this observation is that the polymerization rate is very dependent how fast the initiator is added (or if the initiator is diluted in monomer/solvent, then how concentrated that solution is). This then means that experimental kinetic analysis of ATRP using very efficient initiators needs to be done carefully and in such a way that the mode and rate of initiator addition are reproducible. This also highlights the fact that by changing initiator quite different rates of polymerization can be obtained.

Conclusions

The simulations of ATRP presented here have shown that the kinetics of such polymerizations are complex. The apparent external orders of the reactants (initiator, activator, and deactivator) were found to be often fractional or nonlinear and also depend heavily upon several other factors—primarily the amount of deactivator that is present (or generated) at early stages of the polymerization. If deactivator is present at the beginning of the reaction, then the apparent external orders tend toward unity. Heterogeneity within the polymerization medium was found to also lead to complex kinetics. Using very reactive initiators, such as benzhydryl chloride, may lead to the production of variable amounts of deactivator depending on the mode and rate of addition and therefore affect the rates of polymerization observed.

Acknowledgment. We thank the members of the ATRP Consortium at Carnegie Mellon University for financial support. D.A.S. further acknowledges support from Bayer Corp. through the Bayer Postdoctoral Fellowship at Carnegie Mellon University.

References and Notes

(1) Matyjaszewski, K., Ed. *Controlled Radical Polymerization*; ACS Symp. Ser. Vol. 685; American Chemical Society: Washington, DC, 1998. Matyjaszewski, K. *Chem. Eur. J.* **1998**, *5*, 3095.
(2) Patten, T. E.; Matyjaszewski, K. *Adv. Mater.* **1998**, *10*, 901.
(3) Hawker, C. J. *TRIP* **1996**, *4*, 183.
(4) Matyjaszewski, K.; Gaynor, S.; Wang, J.-S. *Macromolecules* **1995**, *28*, 2093.
(5) Chiefari, J.; Chong, Y. K. B.; Ercole, F.; Krstina, J.; Jeffery, J.; Le, T. P. T.; Mayadunne, R. T. A.; Meijs, G. F.; Moad, C. L.; Moad, G.; Rizzardo, E.; Thang, S. H. *Macromolecules* **1998**, *31*, 5559.
(6) Fischer, H. *Macromolecules* **1997**, *30*, 5666.
(7) Fischer, H. *J. Polym. Sci., Part A: Polym. Chem.* **1999**, 1885.
(8) Shipp, D. A.; Matyjaszewski, K. *Macromolecules* **1999**, *32*, 2948.
(9) Matyjaszewski, K.; Patten, T. E.; Xia, J. *J. Am. Chem. Soc.* **1997**, *119*, 674.
(10) Wang, J.-L.; Grimaud, T.; Matyjaszewski, K. *Macromolecules* **1997**, *30*, 6507.
(11) Davis, K. A.; Paik, H.-J.; Matyjaszewski, K. *Macromolecules* **1999**, *32*, 1767.
(12) Percec, V.; Barboiu, B.; Kim, H.-J. *J. Am. Chem. Soc.* **1998**, *120*, 305.
(13) Pascual, S.; Coutin, B.; Tardi, M.; Polton, A.; Vairon, J.-P. *Macromolecules* **1999**, *32*, 1432.
(14) Wulkow, M. *Macromol. Theory Simul.* **1996**, *5*, 393.
(15) Greszta, D.; Matyjaszewski, K. *Macromolecules* **1996**, *29*, 7661.
(16) Buback, M.; Busch, M.; Lämmel, R. A. *Macromol. Theory Simul.* **1996**, *5*, 845.
(17) Hungenberg, K.-D.; Knoll, K.; Wulkow, M. *Macromol. Theory Simul.* **1997**, *6*, 393.
(18) Müller, A. H. E.; Yan, D.; Wulkow, M. *Macromolecules* **1997**, *30*, 7015.
(19) Griller, D. In *Radical Reaction Rates in Solution* In *Landolt-Bornstein, New Series*; Fischer, H., Ed.; Spring-Verlag: Berlin, 1984; Vol. II/13a, p 5.
(20) Walbiner, M.; Wu, J. Q.; Fischer, H. *Helv. Chim. Acta* **1995**, *78*, 910.
(21) Buback, M.; Gilbert, R. G.; Hutchinson, R. A.; Klumperman, B.; Kuchta, F.-D.; Manders, B. G.; O'Driscoll, K. F.; Russell, G. T.; Schweer, J. *Macromol. Chem. Phys.* **1995**, *196*, 3267.
(22) Berger, K. C.; Meyerhoff, G. In *Rate Constants for Radical Polymerization* In *Polymer Handbook*; Brandup, J., Immergut, E. H., Eds.; Wiley: New York, 1989; p II/67.
(23) Ohno, K.; Goto, A.; Fukuda, T.; Xia, J.; Matyjaszewski, K. *Macromolecules* **1998**, *31*, 2699.
(24) Fischer, H.; Paul, H. *Acc. Chem. Res.* **1987**, *20*, 200.
(25) Hui, A. W.; Hamielec, A. E. *J. Appl. Polym. Sci.* **1972**, *16*, 749.
(26) Griffiths, M. C.; Strauch, J.; Monteiro, M. J.; Gilbert, R. G. *Macromolecules* **1998**, *31*, 7835.
(27) Matyjaszewski, K.; Davis, K.; Patten, T. E.; Wei, M. *Tetrahedron* **1997**, *53*, 15321.
(28) Kajiwara, A.; Matyjaszewski, K.; Kamachi, M. *Macromolecules* **1998**, *31*, 5695.
(29) Wang, J. S.; Matyjaszewski, K. *J. Am. Chem. Soc.* **1995**, *117*, 5614.
(30) Xia, J.; Matyjaszewski, K. *Macromolecules* **1997**, *30*, 7697.
(31) Percec, V.; Barboiu, B.; Neumann, A.; Ronda, J. C.; Zhao, M. *Macromolecules* **1996**, *29*, 3665.
(32) Matyjaszewski, K.; Wang, J.-L.; Grimaud, T.; Shipp, D. A. *Macromolecules* **1998**, *31*, 1527.

MA991651M